NirvaWave: An Accurate and Efficient Near Field Wave Propagation Simulator for 6G and Beyond

Vahid Yazdnian
Electrical Engineering Department
Princeton University
Princeton, USA
vahidyazdnian@princeton.edu

Atsutse Kludze
Electrical Engineering Department
Princeton University
Princeton, USA
kludze@princeton.edu

Yasaman Ghasempour
Electrical Engineering Department
Princeton University
Princeton, USA
ghasempour@princeton.edu

Abstract—The extended near-field range in future mm-Wave and sub-THz wireless networks demands a precise and efficient near-field channel simulator for understanding and optimizing wireless communications in this less-explored regime. This paper presents NirvaWave, a novel near-field channel simulator, built on scalar diffraction theory and Fourier principles, to provide precise wave propagation response in complex wireless mediums under custom user-defined transmitted EM signals. NirvaWave offers an interface for investigating novel near-field wavefronts, e.g., Airy beams, Bessel beams, and the interaction of mmWave and sub-THz signals with obstructions, reflectors, and scatterers. The simulation run-time in NirvaWave is orders of magnitude lower than its EM software counterparts that directly solve Maxwell Equations. Hence, NirvaWave enables a user-friendly interface for large-scale channel simulations required for developing new model-driven and data-driven techniques. We evaluated the performance of NirvaWave through direct comparison with EM simulation software. Finally, we have open-sourced the core codebase of NirvaWave in our GitHub repository.[1]

Index Terms—Near-Field, Simulator, 6G, sub-THz, mmWave

I. INTRODUCTION

Millimeter-wave (mmWave) and Sub-Terahertz (sub-THz) communications are emerging as promising solutions to the spectrum scarcity faced by traditional WiFi and cellular networks [1]. The abundant bandwidth in these frequency bands offers the potential to achieve multi-Gbps data rates essential for immersive extended/virtual reality, high-resolution streaming, intelligent autonomous systems, and ultra-low-latency backhauling [1]. However, the severe propagation loss inherent to this spectral regime necessitates the use of larger apertures for transmitters and receivers, like fixed directional antennas, phased arrays, and reconfigurable intelligent surfaces (RIS), to create highly directional beams to compensate for path loss.

The large array aperture combined with high carrier frequencies in the mmWave and sub-THz bands yields the extension of the near-field region to several meters causing a paradigm shift, i.e., positioning many receivers in the near-field region of the transmitter antennas. Unfortunately, the existing channel simulators are either built on the assumption of planar-wave far-field transmissions or are prohibitively time-consuming for realistic simulations.

[1]The GitHub repository of NirvaWave can be found at https://github.com/vahidyazdnian1378/NirvaWave.

Specifically, EM solvers such as Altair Feko [2] and CST Studio Suite offer accurate EM wave propagation of complex antenna apertures at any frequency and can capture the wave interaction with arbitrarily designed reflectors/obstruction. This is achieved by solving Maxwell's equations using various techniques, including the Method of Moments (MoM), Finite Difference Time Domain (FDTD), and Finite Element Method (FEM) [3]. Although these solvers provide accurate solutions, they lack scalability, as their run-time grows exponentially with the aperture size and the complexity of the wireless medium. Indeed, even simulating simple environments may take up to several hours. Less demanding channel simulators either operate based on statistical channel models (e.g., 3GPP [4] and NYUSIM [5]) or exploit ray tracing methods (e.g., Sionaa developed by NVIDIA [6]). Unfortunately, these schemes do not take into account the spherical wavefront radiated from every element in the transmitting array, and hence are inaccurate in the near-field region. Therefore, developing a precise and efficient near-field channel simulator is crucial for advancing our understanding of mmWave and sub-THz communications in the next-generation wireless networks.

This paper presents NirvaWave, an open-source channel simulator developed for accurate and efficient modeling of electromagnetic wave propagation in near-field wireless settings. NirvaWave leverages the scalar diffraction theory and the Rayleigh-Sommerfeld integral to ensure a high level of accuracy by adhering completely to the fundamental physics of EM wave propagation. To achieve computational efficiency, NirvaWave's core algorithm is built based on the Angular Spectrum Method that exploits Fourier properties. NirvaWave supports free-space and inhomogeneous near-field mediums with blockers and reflectors. The complex electric field at the transmitter (including phase and amplitude per antenna) can be defined by the user. We have implemented emerging near-field wavefronts with unique characteristics as default options. This includes conventional beam shaping schemes such as far-field Gaussian beams and near-field focused beams as well new wavefront like Airy beams [7] with curved trajectories and Bessel beams [8] with the unique property of self-healing, i.e., the wavefront is reconstructed after interacting with obstruction. We emphasize that today's wireless channel simulators do not allow for the implementation of these exotic wavefronts.

Additionally, the simulator supports RIS implementation and can capture scattering off of rough surfaces with wavelength-level height perturbation. Finally, users can define realistic wireless mediums with multiple TXs, RXs, and obstructions and find the received signal heatmap in such complex settings.

We rigorously benchmark NirvaWave EM wave propagation simulations against highly accurate yet computationally demanding EM simulators. Our extensive simulation results demonstrate strong alignment with the ground truth across various environments while reducing the simulation run-time by orders of magnitude. We believe NirvaWave provides a user-friendly interface for studying mmWave and sub-THz near-field channels and will pave the way for developing model-driven and data-driven techniques to address the challenges of wireless communications in these high-frequency regimes.

II. NEAR-FIELD CHANNEL MODELING AND SIMULATOR DESIGN

In this section, we explain the physical principles incorporated into NirvaWave making it capable of accurately and efficiently modeling near-field EM wave propagation. Specifically, we will first explain the Rayleigh-Sommerfeld integral theory that serves as the foundational principle for modeling the radiation of spherical waves in free-space. Then, we extend our modeling to inhomogeneous environments with the presence of blockers and reflectors. We show how small perturbations in the surface of the reflector can cause diffuse scattering and its impact on reflection characteristics. We will also explain the principles of RIS implementation in near-field channels. Finally, we outline the design flow of the simulator and describe NirvaWave's core algorithm.

A. Primer on Rayleigh-Sommerfeld Integral Theory

Assume we have a transmitter array at $x = x_0$, as shown in Fig. 1. The Rayleigh-Sommerfeld theory suggests that we can consider this aperture as an infinite number of point sources each emitting spherical waves. Further, to find the electric field in an arbitrary point (x,y,z), we have to add the contributions from all these point sources together. Since in this theory, there is no assumption about the initial E-field distribution, it allows us to implement any phase/amplitude profile on TX antenna arrays and find the corresponding electric field at arbitrary RX locations or observation planes. The general form of the Rayleigh-Sommerfeld integral can be derived from Maxwell's equations by use of Green's Theorem as follows [9]:

$$E(x', y', z'|E_0) =$$
$$\frac{1}{2\pi} \iint_A E_0(x_0, y, z) \left(\frac{\Delta x \, e^{-ikr}}{r^2} \left(ik + \frac{1}{r} \right) \right) dydz, \quad (1)$$

where, $E(x_0, y, z)$ represents the initial E-field distribution at x_0. This integral theory would find the complex E-field at any arbitrary point (x', y', z'). k represents the wave number, $\Delta x = x' - x_0$, and $r = \sqrt{(x' - x_0)^2 + (y' - y)^2 + (z' - z)^2}$ is the distance from each source point to the desired location.

Although the Rayleigh-Sommerfeld integral provides a straightforward method to find the EM wave evolution as
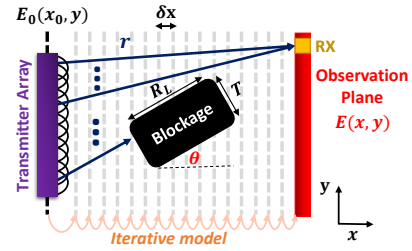

Fig. 1: Demonstration of the iterative Rayleigh-Sommerfeld integral theory that captures the evolution of an arbitrary electric field distribution $E_0(x_0, y)$ in space in the presence of blockers and reflectors.

it propagates between TX and RX, it requires computing a discrete integral at each point in space, which is significantly time-consuming. The Angular Spectrum Method (ASM) simplifies the computation of this integral by transforming the equation into the frequency domain using Fourier principles, leveraging the fact that Eq. (1) can be written in the form of convolution. Particularly, using ASM, we can write:

$$\mathcal{F}\{E(x', y', z'|E_0)\} =$$
$$\mathcal{F}\{E(x_0, y, z)\} \times \mathcal{F}\left\{ \frac{1}{2\pi} \frac{\partial}{\partial x'} \left(\frac{e^{-ikr}}{r} \right) \right\} \quad (2)$$

This way we can interpret the free space propagation as a linear system in which $\mathcal{F}\left\{ \frac{1}{2\pi} \frac{\partial}{\partial x'} \left(\frac{e^{-ikr}}{r} \right) \right\}$ can be viewed as a transfer function that captures the EM disturbance of a point source transmission. In other words, we can write:

$$H(f_y, f_z) = \mathcal{F}\left\{ \frac{1}{2\pi} \frac{\partial}{\partial x'} \left(\frac{e^{-ikr}}{r} \right) \right\} =$$
$$exp(-i2\pi \frac{(x' - x)}{\lambda} \sqrt{1 - \lambda^2 \, (f_y^2 + f_z^2)}), \quad (3)$$

where λ is the wavelength, f_y and f_z represent spatial frequencies. We highlight that the transfer function $H(f_y, f_z)$ is solely a function of the geometry of the environment and not the transmitted electric field. Finally, $E(x', y', z'|E_0)$ can be calculated by taking a Fourier inverse as follows:

$$E(x', y', z'|E_0) = \mathcal{F}^{-1}\left\{ \mathcal{F}\{E(x_0, y, z)\} \times H(f_y, f_z) \right\}. \quad (4)$$

In NirvaWave, we use the simplified 2D version of Eq. (1)-(4). Indeed, Fourier transforms are much more computationally efficient and help reduce the complexity and rum-time of simulations in NirvaWave. However, as mentioned earlier, such calculation only applies to free-space communication and other techniques needed to extend it to a wireless medium that involves blockers and reflectors.

B. Near-Field Blockage Modeling and Simulation

The Rayleigh-Sommerfeld integral theory originally describes EM wave propagation in free space. However, to account for diffraction due to environmental blockages, we must model the relevant boundary conditions. In free space, using the angular spectrum method, we can compute the electric field at each location $x = x'$ either based on the initial E-field at $x = x_0$ in one shot or based on the previously calculated E-field

at $x = x' - \delta x$ using an iterative approach. However, when there are blockages in the environment, we must rely on an iterative scheme to account for any disturbances and discontinuities in the E-field caused by the presence of blockers.

As depicted in Fig. 1, δx represents the discrete step size for iterative calculations, and R_L and T denote blocker length and thickness respectively. In NirvaWave, we use $BL(x, y)$ to characterize arbitrary-shaped blockers. Specifically, if $BL(x, y) = 1$, the signal is unattenuated at point (x, y), indicating no blocker. Conversely, $BL(x, y) = \alpha$, where $0 \leq \alpha < 1$, captures the attenuation constant caused by a blocker at (x,y). Thus, the E-field distribution at the observation plane can be determined through an iterative process with the kth iteration for $x = x_0 + k\delta x$ expressed as:

$$E(x, y) = BL(x, y) \times \mathcal{F}^{-1}\{H(f_y) \times \mathcal{F}\{E(x - \delta x, y)\}\} \quad (5)$$

Using this approach, NirvaWave is able to account for the diffraction behavior of EM wave propagation in the presence of blockages in a time-efficient manner.

C. Near-Field Reflection Modeling and Simulation

For simplicity and without loss of generality, we will first explain how to characterize a single near-field reflector in the environment, followed by a discussion of the general case using a recursive algorithm. To this end, NirvaWave starts by calculating the E-field in the environment assuming there are no reflections. Then, we can find the electric field incident on the reflector's surface denoted as $E(x_{ref}, y_{ref})$, where (x_{ref}, y_{ref}) represents the points on the reflector. Building on top of the Huygens-Fresnel principle [10], we treat the reflector as another source of EM signals in the medium, determined using the previously calculated initial radiating E-field. In other words, similar to modeling the transmitter, we consider the reflector as an infinite number of point sources radiating spherical wavefronts. Therefore, the reflected signal can also be characterized by the Angular Spectrum Method.

It is important to note that ASM originally describes EM wave propagation when the direction of propagation is normal to the E-field source plane. However, when considering reflections, the propagation direction is no longer normal to the reflector plane. Accordingly, the original transfer function described in Eq. (3) must be modified. Indeed, the rotation angle between reflector and virtual source planes (denoted as θ in Fig. 2) is purely a function of reflector orientation relative
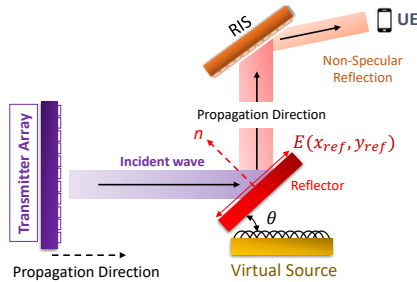

Fig. 2: Demonstration of reflection and reconfigurable intelligent surfaces implementation in NirvaWave.

to TX. Hence, the transfer function in Eq. (3) can be expressed based on full diffraction theory as [9]:

$$H_m(f_y|\theta) = exp(-i2\pi \frac{(x' - x)}{\lambda cos(\theta)} \sqrt{1 - (\lambda f_y cos(\theta))^2}) \quad (6)$$

Therefore, the EM wave propagation of the reflected wave can be derived using Eq. (4) by considering the modified transfer function $H_m(f_y|\theta)$ and the virtual initial EM wave source $E_{vir}(x_0, y) = E(x_{ref}, y_{ref})$. Hence, we can compute the reflected E-field profile in the reflector coordinate system (similar to Eq. (5)) through an iterative process:

$$\begin{aligned} E_{vir}(x, y) = &BL_{ref}(x, y) \times \\ &\mathcal{F}^{-1}\{H_m(f_y|\theta) \times \mathcal{F}\{\Gamma_r \times E_{vir}(x - \delta x, y)\}\} \end{aligned} \quad (7)$$

where $BL_{ref}(x, y)$ denotes the blocker properties in the reflector coordinate system and Γ_r is the reflection coefficient (between 0-1) that can be input by the users. Using this approach, we can model the reflected EM wave propagation in the coordinates of the corresponding reflector plane. Later in Sec. II-F, we will explain how to find the total field propagation considering the contribution of the TX radiation and other potential virtual sources (i.e., reflectors/RISs).

D. Diffuse Rough Scattering Implementation in NirvaWave

In Sec. II-C, we explained how a specular reflection can be captured in NirvaWave. In practice, reflection at high frequencies also includes diffuse scattering components as the small perturbations on the surface of the reflection become comparable with the sub-mm wavelength of the impinging waves. Indeed, past work showed such scattering behavior has important implications for signal coverage and mobility resilience in sub-THz wireless networks [11]. Hence, here we explain how to model rough scattering surfaces in NirvaWave.

Surface perturbations are often modeled with a Gaussian distribution, with height at location (x) as $H(x) \sim \mathcal{N}(0, h_{rms}^2)$, where h_{rms} is the standard deviation of the surface height. Similarly, we can define correlation length Lc as an indicator of horizontal roughness [12]. NirvaWave allows users input (h_{rms}, L_c) parameters that capture the statistical profile of random diffuse scattering to analyze the effects of that on communication systems. Specifically, a generated random height perturbation $H(x, y)$ based on user-defined h_{rms} and L_c values is translated to the corresponding additional phase variation on the suraface as: $\phi_{rough}(x, y; h_{rms}, L_c) = 2\pi \frac{H(x,y)}{\lambda}$. Therefore, the electric field reflected from the surface of a rough object can be approximated as:

$$E_{vir}(x_0, y) = E(x_{ref}, y_{ref}) \times e^{j2\pi \phi_{rough}(x,y;h_{rms},L_c)} \quad (8)$$

Hence, the reflection off of a rough surface can be characterized similar to a smooth reflector, albeit by updating the electric field at the virtual source according to Eq. (8) above.

E. Implemenation of Reconfigurable Surfaces in NirvaWave

Reconfigurable Intelligent Surfaces (RIS) are emerging as a promising technology for future wireless communication systems. RIS employs a large number of low-cost passive

unit cells to intelligently and flexibly control electromagnetic wave properties—such as amplitude, phase, and polarization—thereby optimizing the propagation channel to establish the best possible transmission links. Therefore, implementing near-field channel modeling to analyze THz and sub-THz wireless systems in the presence of RIS would be highly important. To implement RIS, we need to change the phase and amplitude configuration of the calculated E-field on the RIS plane, $E(x_{RIS}, y_{RIS})$, based on the user-defined RIS phase shift and amplitude for each element, denoted by ϕ_{RIS} and A_{RIS}. Specifically, we can write:

$$E_{vir}(x_0, y) = E(x_{RIS}, y_{RIS}) \times A_{RIS} e^{j2\pi\phi_{RIS}} \qquad (9)$$

Using this approach, NirvaWave is able to model EM wave reflection off of the RIS by modifying the reflecting E-field distribution from $E_{vir}(x_0, y)$ to $E(x_{RIS}, y_{RIS})$ in Eq. (7).

F. NirvaWave Recursive Algorithm

Thus far, we have provided the fundamental physical principles to model the near-field EM wave propagation in complex inhomogeneous mediums. Here, we explain the core algorithm of NirvaWave. In general, the environment may include several blockers, reflectors, or RISs. Hence, NirvaWave finds the wave propagation through a recursive algorithm, where the function is called within itself to account for the reflections off of the consecutive reflectors/RIS planes. This recursive algorithm first solves the EM wave propagation based on the initial electric field on the TX array and finds incident E-field on both sides of all reflector/RIS planes. This is done using a list of objects in the field of view and their geometric features. Then, for each reflector/RIS in the environment, the object list is updated using coordinate transformation and the contribution of the reflectors (as virtual sources) is calculated by repeating the same procedure. The algorithm would continue calculating the consecutive reflections until the termination condition is satisfied. Ultimately, the transformed E-fields resulting from the reflections and the TX radiation are recursively summed to obtain the total electric field in the environment.

III. GRAPHICAL USER INTERFACE

We have provided a Graphical User Interface (GUI) to facilitate the study of near-field channel modeling for the next generation of communication systems. Fig. 3 illustrates the GUI main window. We have made the core codebase of the NirvaWave simulator readily accessible in GitHub repository.

A. Input Parameters

In NirvaWave, users can specify various environmental factors, including dimension, resolution, blockages, reflectors, and RISs, as well as the properties of the transmitter (TX) and receiver (RX) antenna arrays, and their phase configurations. We have included a complete instruction of input parameters in the Github repository. The spatial resolution is custom-defined through *Dimension* and *Resolution* inputs. We note that a minimum spatial resolution of $\lambda/2$ is required to correctly capture EM propagation. Users can also define reflectors and

blockages in the environment by specifying their center location, length, orientation, thickness, and reflection coefficient. For rough surfaces, the statistical roughness parameters h_{rms} and L_c can be set. Further, users can configure an RIS into the environment at any location with the desired phase profile.

The GUI allows for configuring the TX antenna properties and the operating frequency. NirvaWave imposes no restrictions on frequency or dimension, as it is accurate in both Near-Field and Far-Field regimes. We emphasize that unlike EM simulators like HFSS and CST that allow for custom antenna geometry and design, NirvaWave is not an antenna simulator. Specifically, we assume ideal isotropic antennas at the transmitter aperture that can adopt any custom phase or amplitude profile by importing a text file, the details of which can be found on the GitHub repository. Additionally, NirvaWave allows for simulations of arbitrary near-field wavefronts, including Bessel beams and Airy beams. Users can also input their custom complex E-field distribution on TX aperture and simulate their behavior in free-space and inhomogeneous mediums. Finally, in NirvaWave users can define multiple RX antenna array properties, including center location, length, orientation, and the number of elements, to calculate the power at the intended UE locations. By default, the RX antenna is assumed to be fully digital. For analog arrays, users should import a text file containing the weight vector configuration.

B. Output Files

The NirvaWave provides an accurate yet efficient wave propagation profile based on the underlying physics principles outlined before. The output involves coverage maps and received power at specified User Equipment (UE) locations. Additionally, the calculated electric field at each location can be saved for further analysis. Examples of radiation maps are provided in Sec. IV.

C. Large Data Dataset Collection

The fast simulation run-time, the ultimate flexibility in transmitted electric fields, and on-demand wireless mediums make NirvaWave a promising tool for data collection at scale. Such
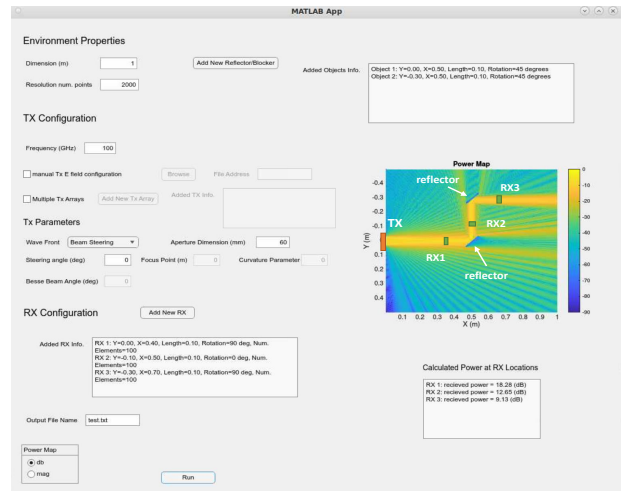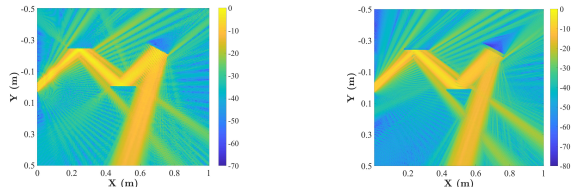
Fig. 3: Graphical User Interface (GUI) of NirvaWave.

(a) Feko coverage map   (b) NirvaWave coverage map

Fig. 4: Coverage map results from NirvaWave and Feko simulations in an environment with three reflectors.
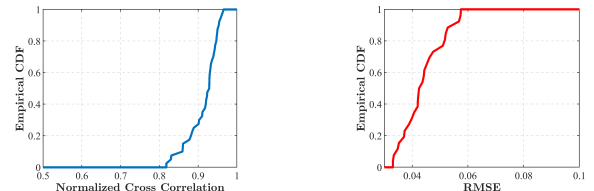
massive data collection plays a pivotal role in deepening our understanding of near-field wireless channels in this untapped territory, as well as developing new data-driven and AI-assisted models that can estimate or predict how EM waves evolve in complex environments. To assist users in getting started, we have included a basic script file in GitHub that serves as a guide. This script can be easily customized to meet the unique requirements of different applications.

IV. SIMULATOR EVALUATION

In this section, we evaluate the performance of the NirvaWave simulator in various environmental configurations and wavefront designs. We compare our result with Altair Feko [2], a sophisticated EM simulation software. It should be noted that the simulation environment in Feko is 3D with 2D antenna apertures. However, we only solve the EM wave propagation in the plane of interest to compare the output results to NirvaWave. We run all the simulations at 100 GHz.

Metric. We exploit two complementary metrics for evaluation purposes. The first metric is Root Mean Squared Error (RMSE), which measures the point-wise difference between the normalized E-field intensities from Feko and NirvaWave, ranging from 0 (no difference) to 1 (maximum difference). The second metric aims to evaluate the structural similarity between the two E-field heatmaps. To this end, we can calculate the 2D cross-correlation of normalized $N \times N$ matrices $|\mathbf{E}_{Feko}|$ and $|\mathbf{E}_{sim}|$, i.e., $\mathbf{R} = |\mathbf{E}_{Feko}| \star |\mathbf{E}_{sim}|$, where $\mathbf{R}$ is a $(2N - 1) \times (2N - 1)$. We use the maximum value in $\mathbf{R}$ as the metric of similarity between coverage maps which ranges from -1 to 1, with 1 showing a perfect match. Hence, a cross-correlation close to 1 demonstrates a higher structural similarity, which RMSE alone cannot capture.

Simulation Run-Time. EM simulation software like Feko that models EM wave propagation by solving Maxwell's equations is accurate, albeit extremely time-consuming in practice. The run-time issue is exacerbated as the number of reflectors or the TX aperture size increases. In a basic environment with two reflectors and a 10 cm TX aperture, the simulation in NirvaWave is over 40 times faster. More importantly, while the runtime of large EM simulators increases exponentially with the TX aperture size, the runtime in NirvaWave remains almost unaffected. For instance, with a 20 cm TX aperture and one reflector, NirvaWave's run time is 200+ times faster than Feko. In more complex environments, the efficiency of NirvaWave compared to EM simulators becomes even more pronounced.

(a) Normalized correlation   (b) RMSE

Fig. 5: Evaluation of NirvaWave accuracy in near-field channel modeling in comparison with Feko in different environments.
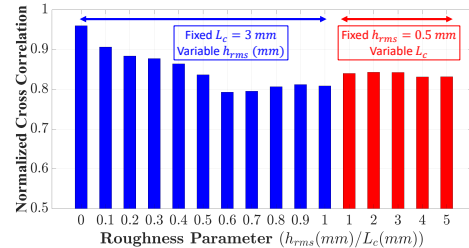

Fig. 6: Normalized cross correlation between NirvaWave and Feko in diffuse scattering simulations. Blue bars represent fixed L_c = 3 mm and variable h_{rms} (mm) while red bars represents fixed h_{rms} = 0.5 mm and variable L_c (mm).

A. Performance of NirvaWave in Reflector Simulations

First, we evaluate the performance of NirvaWave in capturing the near-field channels under the presence of reflectors. We systematically try 40 different environmental configurations such that the reflector is in the near-field of the TX in all cases. We also tested different roughness parameters to assess the performance of NirvaWave under diffuse rough scattering.

1) Specular Reflection: We simulated 18 scenarios with a single reflector, 14 cases with two reflectors, 3 scenarios with three reflectors, 3 environments with a single blocker, and two special cases with non-Gaussian transmitted wavefronts (Airy Wavefront and Bessel Beam). Fig. 4 illustrates the simulation results from NirvaWave and Feko for an environment with three reflectors. We observe that visually the heatmaps match pretty well. Additionally, Fig. 5 presents the empirical CDFs of RMSE and normalized correlation for all 40 configurations. RMSE is under 0.06 for all settings, with 80% achieving below 0.05. Normalized cross-correlation is above 0.8 across all configurations, with 80% exceeding 0.9. The results demonstrate NirvaWave's ability to accurately simulate reflection and blockage for any arbitrary primary electric field distributions.

2) Diffuse Rough Scattering: To simulate diffuse rough scattering, we generate a random height distribution, representing the surface height perturbations, based on a specific pair of h_{rms} and L_c values and import the rough surface into Feko. For simulating the same surface in NirvaWave, we sample the generated height distribution and convert it into corresponding phase shifts on the reflector plane. We conducted 15 simulations with varying roughness parameters: 10 with L_c = 3 mm and varying h_{rms} from 0 to 1 mm, and 5 with h_{rms} = 0.5 mm and varying L_c from 1 to 5 mm. Fig. 6 presents the normalized cross-correlation between the simulations in Feko and NirvaWave for all 15 scenarios. We
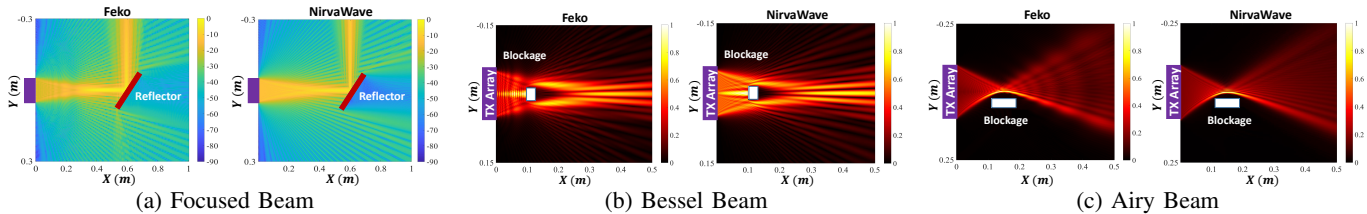
(a) Focused Beam   (b) Bessel Beam   (c) Airy Beam

Fig. 7: Emerging near-field wavefornts simulation results in Feko and NirvaWave.

observe that the normalized cross-correlation exceeds 0.80 in all settings, with an average value of 0.84. These findings demonstrate NirvaWave's capability to accurately capture the diffuse rough scattering phenomenon in the near-field region of the THz Tx antenna arrays. However, as surface roughness increases, the discrepancies between the two simulators slightly grow, mainly due to the increased impact of random diffuse scattering in 3D for rougher surfaces. Nevertheless, for most natural indoor/outdoor surfaces, $h_{rms} < 0.7$ [11].

B. Unique Near-field Wavefronts

One of the unique advantages of NirvaWave is the ability to simulate arbitrary transmit wavefronts, unlike state-of-the-art simulators that solely consider conventional Gaussian beams. Here, we simulate three special near-field wavefronts, namely focused beam, Airy beam, and Bessel beam, to evaluate the performance of NirvaWave in capturing the special characteristics of these wavefronts in inhomogeneous mediums:

(i) First, we implement a focused beam in the presence of a near-field reflector. To this end, we use a 10 cm TX array at 100 GHz yielding a near-field distance of around 3 meters. We place a reflector at $(x, y) = (0.6 \, \text{m}, 0 \, \text{m})$ with $R_L = 0.2$ m and $\theta_r = 45°$, i.e., the reflector is in the near-field of the array. We configure the focused beam to have a focal length of 0.6 m. The results from NirvaWave and Feko in this environment are shown in Fig. 7a. We observe that NirvaWave matches well with EM software Feko. *(ii)* The Bessel beam is emerging due it its non-diffraction properties (in a certain regime) and its self-healing property, which allows the beam to reconstruct even after being blocked by an obstacle [8]. To simulate Bessel beams, we use a TX aperture dimension of 10 cm at 100 GHz and adopt the phase configuration corresponding to a Bessel beam non-diffraction angle [8] of $\alpha = 5°$, with a blockage placed at $(x, y) = (0.1 \, \text{m}, 0 \, \text{m})$. The results from NirvaWave and Feko in this environment are illustrated in Fig. 7b. We observe that the wavefront before and after the obstruction is captured accurately by NirvaWave. *(iii)* Finally, we implemented an Airy beam that has a curved trajectory in space making it an interesting solution to curve around obstacles in the environment and mitigate blockages. We simulate an aperture of size 20 cm at 100 GHz with the Airy phase function [7] to achieve a curvature parameter of $\beta = -4.5$ and a focal length of $f = 0.15$ m. We place a blockage at $(x, y) = (0.15 \, \text{m}, -0.07 \, \text{m})$ with a thickness of 5 cm and a length of $R_L = 0.1$ m. Fig. 7c demonstrates that NirvaWave captures the correct trajectory of near-field waves as they curve around the obstacle.

These results demonstrate NirvaWave's ability to capture the near-field characteristics of important and arbitrary wavefronts in the presence of blockages and reflectors in the wireless setting, which is essential for studying the sub-THz near-field channel for the next generation of communication systems.

V. CONCLUSION

This paper introduces NirvaWave, an open-source simulator developed for modeling near-field EM wave propagation based on scalar diffraction theory. NirvaWave offers a precise and efficient framework for analyzing the near-field propagation and interaction of EM waves in various user-defined wireless mediums incorporating blockers, reflectors, and scatterers. It allows users to set TX antenna array properties and specify the corresponding complex E-field distribution either through arbitrary user-defined inputs or by selecting from a range of implemented emerging near-field wavefronts. With its user-friendly interface, NirvaWave facilitates the study of mmWave and sub-THz near-field channels while ensuring efficiency, scalability, and accuracy, paving the way for the development of model-driven and data-driven techniques to address the challenges of wireless communications in these high-frequency regimes.

REFERENCES

[1] H. Tataria, M. Shafi, A. F. Molisch, M. Dohler, H. Sjöland, and F. Tufvesson, "6g wireless systems: Vision, requirements, challenges, insights, and opportunities," *Proceedings of the IEEE*, 2021.

[2] I. Altair Engineering, "Altair feko website," https://altair.com/feko.

[3] C. A. Balanis, *Advanced Engineering Electromagnetics*. Wiley, 2016.

[4] M. K. Samimi and T. S. Rappaport, "Local Multipath Model Parameters for Generating 5G Millimeter-Wave 3GPP-like Channel Impulse Response," in *European Conference on Antennas and Propagation*, 2016.

[5] S. Sun, G. R. MacCartney, and T. S. Rappaport, "A Novel Millimeter-Wave Channel Simulator and Applications for 5G Wireless Communications," in *IEEE international conference on communications*, 2017.

[6] J. Hoydis, F. A. Aoudia, S. Cammerer, M. Nimier-David, N. Binder, G. Marcus, and A. Keller, "Sionna RT: Differentiable Ray Tracing for Radio Propagation Modeling," in *IEEE Globecom Workshops*, 2023.

[7] T. Latychevskaia, D. Schachtler, and H.-W. Fink, "Creating airy beams employing a transmissive spatial light modulator," *Applied optics*, 2016.

[8] A. Singh, I. V. Reddy, D. Bodet, and J. M. Jornet, "Bessel beams for 6g-a performance analysis," in *Asilomar Conference on Signals, Systems, and Computers*, 2022.

[9] N. Delen and B. Hooker, "Free-space beam propagation between arbitrarily oriented planes based on full diffraction theory: a fast fourier transform approach," *JOSA A*, 1998.

[10] F. Depasse, M. Paesler, D. Courjon, and J. Vigoureux, "Huygens–fresnel principle in the near field," *Optics letters*, 1995.

[11] R. Shen and Y. Ghasempour, "Scattering from rough surfaces in 100+ ghz wireless mobile networks: From theory to experiments," in *ACM MobiCom*, 2023.

[12] A. K. Fung, "Microwave scattering and emission models and their applications," 1994.